Role of Multiparametric Ultrasound in Determining the Presence of Tumor-Infiltrating Lymphocytes in Invasive Breast Cancer

Insights From B-Mode, SWE, and SMI Modalities

Yasemin Kayadibi, MD, Gul Esen, MD, Seda Aladag Kurt, MD, Ceyda Sönmez Wetherilt, MD, Tulin Ozturk, MD, Yasemin Nur Icten, Fusun Taskin, MD

Received May 13, 2025, from the Department of Radiology, Istanbul University-Cerrahpasa, Cerrahpasa Medical Faculty, Istanbul, Turkey (Y.K., S.A.K.); Senology Research Institute, Acibadem Mehmet Ali Aydinlar University, Istanbul, Turkey (G.E., F.T.); Department of Pathology, Istanbul University-Cerrahpasa, Cerrahpasa Medical Faculty, Istanbul, Turkey (C.S.W., T.O.); and Enka High School, Istanbul, Turkey (Y.N.I.). Manuscript accepted for publication July 24, 2025.

[Correction added on 20 August 2025, after first online publication: The copyright line was changed.]

Address correspondence to Yasemin Kayadibi, Department of Radiology, Istanbul University-Cerrahpasa, Cerrahpasa Medical Faculty, Kocamustafapasa, Istanbul, Turkey.

E-mail: yasemin.kayadibi@iuc.edu.tr

Abbreviations

BI-RADS, Breast Imaging Reporting and Data Systems; CEUS, contrast-enhanced ultrasound; SMI, superb microvascular imaging; SWE, shear wave elastography; TIL, tumor infiltrating lymphocytes; TNBC, triple-negative breast cancer; US, ultrasonography; VI, vascular index

doi:10.1002/jum.70022

Objective—To evaluate the relationship between tumor-infiltrating lymphocyte (TIL) levels and multiparametric ultrasonography (US) findings combining B-mode US, shear wave elastography (SWE), and superb microvascular imaging (SMI) in patients with invasive breast cancer, and to explore the potential of sonographic imaging modalities in predicting the tumor immune microenvironment.

Methods—This retrospective study included 148 patients diagnosed with invasive breast carcinoma between September 2021 and December 2024. Patient age, medical history, and immunohistopathological characteristics (grade, hormone positivity, Ki-67 ratio, subtype) of the lesions were recorded. TIL levels were assessed on hematoxylin–eosin (H&E) stained slides by pathologists following the International TILs Working Group guidelines, and lesions were categorized by different TIL levels (presence/absence, ≥10%, ≥20%, ≥30%). US evaluations were performed using a Toshiba Aplio A system (Canon, Tokyo, Japan) with a 12–16 MHz breast probe. Imaging assessments included B-mode ultrasound (morphology, echogenic halo sign), SWE (*E*-mean, *E*-ratio, stiff rim sign), and SMI (Adler classification, SMI vascular index). Associations between TIL levels and imaging parameters were analyzed using Chi-square tests for categorical and Student's *t*-tests for continuous variables (SWE and SMI).

Results—TIL was detected in 121 of 148 lesions (81.8%). TIL value was >10% in 33 lesions, >20% in 12, and >30% in 8 lesions. On B-mode US, round/oval tumor shape ($p = .003$ at level of TIL > 20%, $p = .001$ at level of TIL > 30%) and non-parallel orientation ($p = .023$) were more prevalent in TIL positive lesions. On SWE, tumors with TIL levels ≥10% were significantly associated with higher *E*-mean values (130 ± 24.7 vs. 107.9 ± 36, $p = .001$) and the presence of a stiff rim sign ($p < .001$). Penetrating vascular structures were more commonly observed on SMI in lesions with TIL ≥ 10% ($p = .023$), along with a higher mean vascular index ($p = .036$). No significant difference was found in other US-SWE and SMI findings (all $p > .4$).

Conclusion—Our findings suggest that US features, particularly vascularity on SMI and stiffness on SWE, may reflect TIL presence in breast cancer. However, methodological variations and differing TIL levels across studies may influence inconsistent associations, especially with SWE. Further comprehensive studies are needed to clarify this relationship.

Key Words—breast cancer; immuno-oncology; shear wave elastography; superb microvascular imaging; tumor-infiltrating lymphocytes; ultrasound

Tumor-infiltrating lymphocytes (TILs) are a critical component of the tumor immune microenvironment, and TIL level has gained increasing attention as a prognostic and predictive biomarker in breast cancer. High TIL levels have been associated with better response to chemotherapy and improved outcomes, particularly in aggressive subtypes such as HER-2 positive and triple-negative breast cancers (TNBC).[1–3] However, findings remain inconsistent in luminal-type tumors (hormone receptor-positive and HER-2 negative).[4–6] Breast cancer exhibits substantial heterogeneity in terms of prognosis. In addition to established prognostic markers such as Ki-67 index, lymphovascular invasion, and tumor size, the preoperative assessment of stromal TILs may play a significant role in guiding oncological treatment decisions.[7–9] TIL levels are traditionally assessed through histopathological evaluation of surgical or biopsy specimens. However, due to the heterogeneous distribution of lymphocytic infiltration within the tumor tissue, limited biopsy samples may not accurately reflect the true TIL density.[10,11] Although the non-invasive nature and widespread availability of radiological imaging methods offer significant clinical advantages, the extent to which these methods can reliably predict TIL density in different tumor types remains unclear. Therefore, there is increasing research on estimating TIL density in breast cancer noninvasively using radiological methods.[12]

Recent studies have focused on the relationship between TIL levels and radiological imaging features in breast cancer.[12] TIL-positive tumors are usually oval or round, well-circumscribed, and have heterogeneous internal structures, as well as posterior acoustic enhancement.[13–15] On MRI, these tumors are characterized by homogeneous contrast enhancement, washout patterns, and low ADC values.[12,14,16] These findings demonstrate that TIL presence can be predicted using non-invasive methods and may aid in predicting treatment response. However, it is noteworthy that each of these TIL studies has used different TIL levels when defining lymphocyte-rich tumors.[12]

Recent advances in ultrasonography (US) techniques, including shear wave elastography (SWE) and superb microvascular imaging (SMI), have enabled more detailed characterization of tumor stiffness and vascularity.[17,18] SWE is a non-invasive complementary technique to B-mode US in distinguishing between benign and malignant lesions by determining the tissue stiffness.[17,19,20] In addition to classical ultrasound findings, SWE can also provide information about tumor aggressiveness, molecular subtype, and treatment response.[17,21–24] High elasticity values have been shown to correlate with high tumor grade, HER-2 positivity, and poor prognostic factors in breast cancer.[22,25,26] Studies conducted in breast cancer have yielded conflicting results between TIL levels and tumor stiffness measured by SWE.[14,23,27,28] While some studies have not found a significant relationship, others have shown a negative correlation.[14,28] In particular, in the study with the largest number of patients, Eun et al have reported that tumors with high TIL levels had lower elasticity values.[28] However, in these studies, different TIL values were taken as thresholds, limiting the results' comparability. Therefore, studies with different TIL classifications are needed to adapt the findings on the elastography–TIL relationship to clinical applications.

SMI is an advanced US technique that enables the visualization of low-velocity blood flow and fine microvascular structures, surpassing the sensitivity of conventional Doppler imaging. SMI is a promising imaging method for the noninvasive evaluation of tumor microvascularity in breast cancer.[18,29] Studies have reported that microvascular patterns obtained with SMI have significant relationships with prognostic factors such as tumor histological subtype, hormone receptor status, proliferative activity (Ki-67) and microvascular density.[30–32] However, large multicenter studies are needed to standardize this relationship and integrate it into clinical use. The relationship with TIL levels has not been investigated before.

This study aims to examine the relationship between TIL density and US, SWE, and SMI findings in patients with invasive breast cancer. A

multiparametric US approach that includes these three imaging modalities (US, SMI, and SWE) has not been reported before. Moreover, different levels of TIL values were used in different studies, making comparison difficult. In this respect, our study adds a new viewpoint to the interpretation of imaging features at varying TIL levels.

Materials and Methods

Study Design and Population

Our study was carried out prospectively after obtaining approval from the ethics committee of our hospital. All patients with Breast Imaging Reporting and Data Systems (BI-RADS) category 5 lesions, who were referred for US-guided biopsy to our clinic between September 2021 and December 2024, were evaluated with B-mode US, SWE, and SMI before the biopsy procedure. US features were recorded, and all images were saved on PACS. The largest lesion was evaluated in patients with more than one lesion. Only patients with a diagnosis of invasive breast cancer who presented with mass lesions were included in this study. Patients with non-mass lesions on US examination, patients with a previous history of breast cancer treatment (surgery or neoadjuvant chemotherapy) and male patients were excluded. Clinical data and histopathological findings were collected from institutional medical records. Informed oral and written consent was obtained from all patients.

Radiological Evaluation Protocol

US was performed by one of two breast radiologists (S.A.K. with 10 years and Y.K with 12 years of elastography experience in breast imaging) using a Toshiba Aplio A US machine (Canon, Tokyo, Japan) with a breast dedicated probe in the 12–16 MHz range. B-mode findings were evaluated according to BI-RADS 2013 edition.[33] Size (measured on at least two orthogonal planes), shape, margins, orientation, echo characteristics of the largest mass lesion, as well as the presence of halo sign were recorded. SWE and SMI evaluations were also performed using the same Toshiba Aplio A device.

In SWE mode of the device, the tissue stiffness was represented from dark blue (indicating the lowest stiffness) to red (indicating the highest stiffness) within a range of 0–200 kPa. Black regions in the SWE image indicated areas where no shear-waves were detected or tissue stiffness was excessive. When such areas were detected, the image quality was checked using the propagation map. If the shear-waves were not parallel to each other and distorted, the process was repeated until the desired image quality was obtained. Region of interest (ROI) placement was performed by the evaluating radiologist during image acquisition, without prior knowledge of the lesion's histopathological characteristics or TIL level. ROIs were specifically positioned in the stiffest areas of the lesion. At least two orthogonal elastography images were obtained for each lesion, and three ROIs (2×2 mm in diameter) were placed in the hardest (highest elasticity) areas within or adjacent to the lesion. In SWE, parameters that can be measured can vary from device to device. These parameters are *E*-mean (average elasticity measured within the ROI), *E*-max, *E*-min (highest and lowest elasticity values, respectively), and *E*-SD (standard deviation of elasticity, a measurement of intra-tissue heterogeneity). Our device can only measure the *E*-mean value. Therefore, the quantitative parameters used in this study were *E*-mean and *E*-ratio, which is the ratio of the elasticity measurements obtained from the lesion and the adjacent parenchyma. The presence or absence of the "stiff rim" sign, a qualitative parameter in SWE, was also evaluated through consensus reading, blinded to histopathological results. During SWE, care was taken not to apply too much manual compression, and the patients held their breath for 5 s during the procedure to avoid being affected by movement.

The SMI mode was activated to assess the vascularization of the lesions. Imaging parameters were set as follows: velocity scale of 1.5–2.5 cm/s, mechanical index of 1.5, wall filter between 50 and 100 Hz, and a frame rate exceeding 50 Hz. To prevent the collapse of microvessels, the examination was performed with ample application of ultrasound gel and without applying transducer pressure. Images were acquired from the scan plan exhibiting the most prominent vascularity, and the ROI was drawn manually by tracing the lesion borders. Quantitative assessment of vascularity was performed using the SMI vascular index (VI), defined as the percentage ratio of Doppler signal pixels to the total number of pixels within the lesion. In addition, vascular patterns were qualitatively

classified according to Adler's grading system (Grade 0 = no flow, Grade 1 = minimal flow, Grade 2 = moderate flow, Grade 3 = marked flow).[34] In Adler's scoring, the final score was determined by the consensus of the two radiologists in the study. For the purposes of statistical analysis, lesions with Adler Grades 0–1 were categorized as low vascularity, while those with Grades 2–3 were considered highly vascularized. Vascular morphology (classified as simple or complex), vascular distribution (central or peripheral), and the presence of penetrating vessels were systematically documented.

Histopathological Evaluation of Tissue Samples

Following the US examinations, US-guided core needle biopsies were performed (typically 4–5 specimens per lesion) using a 14-gauge automated biopsy needle (Geotek, Ankara, Turkey). TIL values were evaluated on pre-treatment biopsy specimens. Based on the findings of elastography and SMI, care was taken to sample the lesions in a way that best reflected their heterogeneous structure. In addition, the peripheral regions of the lesion were included in the sampling process to ensure that the specimens included the tissue around the tumor.

Histological type, grade, axillary status, hormone receptor levels, HER-2 positivity (FISH staining was also added if necessary) and Ki-67 values were recorded from the pathology reports. Molecular subtypes were determined according to the immunohistochemical staining characteristics of the tumor (positivity of estrogen receptor progesterone receptor, HER-2, and level of Ki-67). The lesions were divided into two groups as hormone receptor (HR) (+) and HR (−). Cases with estrogen receptor positive and/or progesterone receptor positive were considered HR (+) and classified as luminal groups. Lesions expressing only HR with a low Ki-67 value (<14%) were considered luminal A, while those with a high Ki-67 value (>14%) with or without HER-2 positivity were classified as luminal B. HR (−) but HER-2 (+) tumors were classified as HER-2 (+) type, and HR (−) and HER-2 (−) cases were classified as TNBC.[35] The TIL status for each patient was assessed by a single experienced breast pathologist (T.O.) following the guidelines provided by the International Immuno-Oncology Biomarker Working Group on Breast Cancer.[36] According to this guideline, TILs should be evaluated by assessing lymphocytic infiltration in the stromal compartment, specifically, the supportive connective tissue between tumor cells within the tumor mass. In the evaluation, only stromal TILs should be reported, expressed as the percentage of the stromal area occupied by mononuclear inflammatory cells within the intratumoral stroma. TILs must be assessed strictly within the borders of the invasive tumor. Surrounding tissue, areas of necrosis, artefacts, and in situ carcinoma components are excluded during the assessment. Scoring is performed by estimating the percentage of lymphocytes in the stromal area; for example, "TILs 20%" indicates that 20% of the stroma is infiltrated with lymphocytes. This percentage is calculated based on area, not on the number of stromal cell nuclei. Although the TIL level is evaluated as a continuous variable rather than with discrete categories, level values are used in most of the studies for clinical correlation purposes. According to this classification, <10% is considered low, 10–49% is considered moderate, and ≥50% is considered high TIL level.[10] TILs were scored in 10% increments (e.g., present/absent, 10%, 20%, 30%, etc.) in this study. The optimal threshold value for TILs has not yet been clearly defined in studies.[14,16,28,37]

Statistical Analysis

Normality was checked by drawing Shapiro–Wilk or single-sample Kolmogorov–Smirnov tests, histogram, Q–Q plot, and box plot graphs. Data were given as mean, standard deviation, median, minimum, maximum, frequency, and percentage. Nominal variables were analyzed with appropriate Chi-square tests based on expected values. In addition, the continuous data obtained with SMI and SWE were analyzed with the Student's t test. The limit of significance was taken as $p < .05$ and bidirectional. Statistical analyses were performed by using SPSS for Windows, version 20.0 (SPSS Inc., Chicago, IL). To explore the impact of TIL values on radiological findings, we employed various TIL levels to examine how changes in TIL levels influenced radiological outcomes.

Results

Exactly 148 patients with invasive breast cancer were included in this study. The mean age was

54 ± 12.3 years, and the average lesion size was 22.5 ± 11.3 mm. Axillary lymph node status, tumor grades, ER, PR, and HER-2 positivity rates, Ki-67 levels, and molecular subtypes can be seen in Table 1. Although TILs were detected in 121 of 148 patients (81.8%), the rate was above 10% in 33 patients, above 20% in 12 patients, and above 30% in only 8 patients. Mean TIL level was 6.9% ± 12 (Table 1). There was no statistically significant association between TIL levels and patient age ($p = .691$ for TIL presence; $p = .110$ for TIL ≥ 10%; $p = .238$ for TIL ≥ 20%; $p = .956$ for TIL ≥ 30%). Similarly, no significant associations were observed between TIL levels and tumor size ($p = .258$; $p = .553$; $p = .082$; $p = .509$), axillary lymph node status ($p = .771$; $p = .775$; $p = .515$; $p = .417$), histological grade ($p = .403$; $p = .067$; $p = .074$; $p = .315$), or Ki-67 levels ($p = .197$; $p = .118$; $p = .345$; $p = .925$) at increasing TIL levels (presence, ≥10%, ≥20%, ≥30%, respectively). Although TILs were present in 82.6% (100/125) of estrogen receptor (+) lesions, a significant inverse relationship with ER positivity was found at all levels of TILs (>10% ($p = .035$), >20% ($p = .009$), and >30% ($p = .041$)). A significant inverse relationship was found for PR positivity only at a level of >20% ($p = .017$). No significant relationship was observed between HER-2 positivity and the presence of TILs ($p = .375$); however, HER-2 positivity was significantly more frequent in cases with TIL level > 10% ($p = .013$). There was no significant relationship at increasing TIL levels ($p = .151$ for ≥20%, $p = .112$ for ≥30%). In terms of molecular subtypes, no significant difference was found between the groups in terms of the presence of TIL ($p = .064$); however, as the TIL level increased, a significant decrease was observed in the frequency of Luminal A and B subtypes (TIL >10%, $p = .017$; >20%, $p = .020$; >30%, $p = .005$). The findings are presented in detail in Table 2.

Table 1. The Demographical, Clinical, and Histopathological Characteristics of the Patients ($n = 148$)

	Number (%)
Age (years) (mean ± SD)	54 ± 12.3
Lesion size (mm) (mean ± SD)	22.5 ± 11.3
Axillary lymph node metastasis	
Absent	73 (50.7%)
Present	75 (49.3%)
Histological grade	
1	4 (2.7%)
2	79 (53.4%)
3	65 (43.9)
ER status	
Negative	23 (15.5%)
Positive	125 (84.5%)
PR status	
Negative	26 (17.6%)
Positive	122 (82.4%)
Her-2 receptor status	
Negative	38 (25.7%)
Positive	110 (74.3%)
Ki-67 index	
<14%	125 (84.5%)
>14%	23 (15.5%)
Subtypes	
Luminal A	38 (25.7%)
Luminal B	86 (58.1%)
Her-2 (+)	12 (8.1%)
Triple negative	12 (8.1%)
Mean TIL level	6.9% ± 12
TIL positivity	121 (81.8%)
>10%	33 (22.3%)
>20%	12 (8.1%)
>30%	8 (5.4%)

Abbreviations: ER, estrogen receptor; PR, progesterone receptor; TIL, tumor infiltrating lymphocyte.

In B-mode US findings, only orientation and tumor shape showed a significant association with TIL positivity. Round-oval shape showed a significant relationship with TIL positivity at the 20% level (21/136 vs. 6/12, $p = .003$) and at the 30% level (22/140 vs. 5/8, $p = .001$). However, there was no significant difference between lesions with or without TIL positivity (5/27 vs. 22/121, $p = .967$) or at the 10% level (19/115 vs. 8/33, $p = .311$). Non-parallel orientation was detected in 72/121 (59.5%) of TIL-positive lesions and 9/27 (33.3%) of TIL-negative lesions, and the difference was statistically significant ($p = .023$). However, this association lost significance at levels of 10% (16/33), 20% (4/12), and 30% (2/8).

When the margins were evaluated, circumscribed margins were observed in 12/121 (10%) of TIL-positive cases and 2/27 (7.4%) of TIL-negative cases, but the difference was not significant ($p = .687$); it approached the significance limit at the 30% level (2/8, 25%, vs 11/136, 8%, $p = .055$). A hypoechoic echo pattern was observed in 83/121 (68.6%) of TIL-positive cases and in 14/27 (51.9%) of TIL-

Table 2. Comparison of TIL levels with clinical and histopathological findings

	TIL			TIL (10%)			TIL (20%)			TIL (30%)		
	TIL (−) ($n = 27$)	TIL (+) ($n = 121$)	p	TIL (<) ($n = 115$)	TIL (>) ($n = 33$)	p	TIL (<) ($n = 136$)	TIL (>) ($n = 12$)	p	TIL (<) ($n = 140$)	TIL (>) ($n = 8$)	p
Age	54.9 ± 12.3	53.9 ± 12.3	.691	54.9 ± 12	51 ± 12.3	.110	54.4 ± 12	50 ± 13.4		54.1 ± 12.2	53.8 ± 14.2	.956
Size	20.9 ± 8	23 ± 12	.258	22.2 ± 11.7	23.6 ± 9.8	.553	22 ± 11.3	28 ± 10.6		22.4 ± 11.4	25.1 ± 10.5	.509
Axillary lymph node (+)	14 (19.2%)	59 (80.8%)	.771	56 (76.7%)	17 (23.3%)	.775	66 (48.5%)	7 (58.3%)		68 (48.6%)	5 (62.5%)	.417
Grade												
Grade 1	0	4 (3.3%)	.403	4 (3.4%)	0	.067	4 (3%)	0	.074	4 (2.8%)	0	.315
Grade 2	17 (63%)	62 (51.2%)		66 (57.4%)	13 (39.3%)		76 (55.9%)	3 (25%)		77 (55%)	2 (25%)	
Grade 3	10 (37%)	55 (45.5%)		45 (39%)	20 (60.6%)		56 (41%)	9 (75%)		60 (42.8%)	5 (62%)	
Hormone receptor												
ER (+)	25 (92.6%)	100 (82.6%)	.197	101 (87.8%)	24 (72.7%)	.035*	118 (86.7%)	7 (58.3%)	.009*	121 (85.7%)	4 (50%)	.041*
PR (+)	24 (88.9%)	99 (81.8%)	.375	99 (86%)	24 (72.7%)	.071	116 (85.3%)	7 (58.3%)	.017*	119 (86%)	4 (50%)	.060
HER-2 (+)	18 (66.7%)	92 (76%)	.314	80 (69.5%)	30 (90.9%)	.013*	99 (72.8%)	11 (91.6%)	.151	103 (73.6%)	7 (87.5%)	.112
Ki-67% (>14%)	2 (7.4%)	21 (17.3%)	.197	15 (13%)	8 (24.2%)	.118	20 (15%)	3 (25%)	.345	22 (15.7%)	1 (12.5%)	.925
Subtype												
Lum A	11 (40.7%)	27 (22.3%)	.064	35 (30.4%)	3 (9%)	.017*	37 (27%)	1 (8.3%)	.020*	37 (26.4%)	1 (12.5%)	.005**
Lum B	11 (40.7%)	75 (62%)		65 (56.5%)	21 (63.6%)		81 (60%)	5 (41.6%)		84 (60%)	2 (25%)	
HER-2	4 (14.8%)	8 (6.6%)		6 (5.2%)	6 (18.2%)		8 (5.8%)	4 (33.3%)		9 (6.4%)	3 (37.5%)	
TNBC	1 (3.7%)	11 (9%)		9 (7.8%)	3 (9%)		10 (7.3%)	2 (16.7%)		11 (7.8%)	1 (12.5%)	

Abbreviations: ER, estrogen receptor; Lum A, luminal type A; Lum B, luminal type B; PR, progesterone receptor; TIL, tumor infiltrating lymphocyte; TNBC, triple negative breast cancer. *$p < 0.05$; **$p < 0.005$.

negative cases, with the difference not exceeding the statistical limit ($p = .098$). No significant statistical difference was found at increasing levels. Posterior acoustic shadowing was observed in 109/121 (90.1%) of TIL-positive and 25/27 (92.6%) of TIL-negative patients, but the difference was not statistically significant ($p = .687$); however, the trend approached statistical significance at the 20% level (9/12, 75% vs 125/136, 92%, $p = .055$). The presence of an echogenic halo was observed in 36/121 (29.7%) of TIL-positive and 6/27 (22.2%) of TIL-negative patients ($p = .433$). No significant statistical difference was found at increasing levels. Thus, in our study, only non-parallel orientation and round-oval shape were shown to be associated with higher TIL density at certain levels; no statistically significant differences were found in other B-mode parameters (Table 3).

The findings related to using SMI and SWE are presented in Table 4. A significant relationship was found between the presence of penetrating vascular structures and TIL status at SMI. Penetrating vascular structures were significantly more common in TIL-positive tumors (72/121, 59.5%), whereas this rate was lower (9/27, 33.3%) in the TIL-negative group ($p = .023$). However, no significant statistical difference was found at increasing levels (all $p > .7$). In terms of vascular morphology, complex vascular structures were observed more frequently in TIL-positive cases (54/121, 44.7%) compared with TIL-negative cases (10/27, 37%). Still, this difference was not significant in the overall group ($p = .472$) and showed a tendency toward significance only at the 30% level (6/8, 75% vs 58/140, 41.5%, $p = .053$). Vascular distribution was not significantly different between the groups in both peripheral and central distribution. Adler's score was also not significantly associated with TIL levels (all $p > .1$). On the other hand, the mean VI value was higher in TIL-positive tumors (6.57 ± 6.2 vs 3.97 ± 5.4), and this difference was statistically significant ($p = .036$); however, this significance was not maintained in increasing levels.

In SWE findings, *E*-mean value was found to be significant only at the 10% TIL level (*E*-mean: 130 ± 24.7 vs 107.9 ± 36; *E*-ratio: 14.6 ± 7.4 vs 12.2 ± 12.7; $p = .001$). The *E*-ratio did not demonstrate statistical significance in any of the TIL subgroups (all $p > .4$). The presence of the stiff rim sign was significantly associated with TILs at the 10% TIL level (29/33, 87.9% vs 47/115, 41%; $p < .001$). However, this difference was not statistically significant in the other TIL levels (all $p > .05$). Figures 1 and 2 present lesion examples highlighting key imaging features associated with TILs, including peritumoral stiffness on SWE and increased microvascularity on SMI.

Discussion

In this study, we investigated the relationship between TIL levels and multiple US-based imaging parameters, including B-mode US, SWE, and SMI in patients with invasive breast cancer. Our study demonstrated that, among B-mode US features, non-parallel orientation (based on presence vs absence) and a round or oval shape (at 20% and 30% stromal TIL levels) were significantly associated with higher TIL density. These results are partially consistent with prior studies. Studies comparing TIL levels with B-mode US findings have shown that TIL-positive tumors often exhibit benign-appearing features.[12] Fukui et al. (at 50% level)[13] and Candelaria et al.[15] (20% level) reported an association between high TIL levels and US findings, such as oval/round shape, smooth or lobulated margins, and posterior acoustic enhancement.[1] Similarly, Jia et al. observed an association between high TIL levels (>10% level) and posterior enhancement, which may reflect stromal loosening.[38] However, in our study, no significant associations were observed with other B-mode features, such as margins, echogenicity, posterior acoustic shadowing, or the presence of a halo sign, except for a borderline trend in shadowing at the 20% level.

In terms of SWE findings, a significant association was observed between increased *E*-mean and TIL at the 10% level, and the presence of the stiff rim sign was also significantly higher in this group. Previous studies have reported conflicting results regarding the relationship between tumor stiffness and TIL levels.[14,23,27,28] These studies evaluated TIL values at different levels (Çelebi et al. >10%, Li et al. >50%, Lee et al. >30%, Eun et al. >50%).[14,23,27,28] While Çelebi et al.[14] and Li et al.[23] found no correlation with elastography features, Lee et al.[27] reported that low TIL values were associated with high SWE values

Table 3. Comparison of TIL Levels With B-Mode US Findings

	TIL			TIL (10%)			TIL (20%)			TIL (30%)		
	TIL (−) ($n = 27$)	TIL (+) ($n = 121$)	*p*	TIL (<) ($n = 115$)	TIL (>) ($n = 33$)	*p*	TIL (<) ($n = 136$)	TIL (>) ($n = 12$)	*p*	TIL (<) ($n = 140$)	TIL (>) ($n = 8$)	*p*
Shape												
Round-oval	5 (18.5%)	22 (18.18%)	.967	19 (16.5%)	8 (24.25%)	.311	21 (15.4%)	6 (50%)	.003*	22 (15.7%)	5 (62.5%)	.001**
Irregular	22 (81.5%)	99 (81.8%)		96 (83.5%)	25 (75.75%)		115 (84.6%)	6 (50%)		119 (85%)	3 (37.5%)	
Margin												
Circumscribed	2 (7.4%)	12 (10%)	.687	9 (7.8%)	5 (15.15%)	.205	11 (8%)	3 (25%)	.055	12 (8.6%)	2 (25%)	.077
Not circumscribed	25 (92.6%)	109 (90%)		106 (92.17%)	28 (84.85%)		125 (92%)	9 (75%)		128 (91.4%)	6 (75%)	
Echo pattern												
Iso-hyperechoic	13 (48.1%)	38 (31.4%)	.098	41 (35.65%)	10 (3%)	.569	45 (33%)	6 (50%)	.237	48 (34.3%)	4 (50%)	.632
Hypoechoic	14 (51.9%)	83 (68.6%)		74 (64.34%)	23 (69.7%)		91 (66.7%)	6 (50%)		92 (65.7%)	4 (50%)	
Posterior features												
No-enhancement	2 (7.4%)	12 (9.9%)	.687	9 (7.8%)	5 (15.2%)	.205	11 (8%)	3 (25%)	.055	12 (8.5%)	3 (37.5%)	.077
Shadowing	25 (92.6%)	109 (90.1%)		106 (92.2%)	28 (84.5%)		125 (92%)	9 (75%)		128 (91.4%)	5 (62.5%)	
Orientation												
Parallel	18 (66.7%)	49 (40.5%)	.023*	50 (43.5%)	17 (51.5%)	.414	59 (43.4%)	8 (66.7%)	.120	60 (42.8%)	6 (75%)	.070
Not-parallel	9 (33.3%)	72 (59.5%)		65 (56.5%)	16 (48.5%)		77 (56.6%)	4 (33.3%)		80 (57.2%)	2 (25%)	
Echogenic halo sign												
Absent	21 (77.8%)	85 (70.3%)	.433	84 (73%)	22 (66.7%)	.474	97 (71.3%)	9 (75%)	.787	100 (71.4%)	5 (62.5%)	.991
Present	6 (22.2%)	36 (29.7%)		31 (27%)	11 (33.3%)		39 (28.7%)	3 (25%)		40 (28.6%)	3 (37.5%)	

TIL, Tumor infiltating lymphocyte;
*<0.05;
**<0.005.

Table 4. Comparison of TIL Levels With SMI and SWE Findings

	TIL			TIL (10%)			TIL (20%)			TIL (30%)		
SMI findings	**TIL (−) (*n* = 27)**	**TIL (+) (*n* = 121)**	***p***	**TIL (<) (*n* = 115)**	**TIL (>) (*n* = 33)**	***p***	**TIL (<) (*n* = 136)**	**TIL (>) (*n* = 12)**	***p***	**TIL (<) (*n* = 140)**	**TIL (>) (*n* = 8)**	***p***
Morphology												
Simple	17 (63%)	67 (55.3%)	.472	68 (59%)	16 (48.5%)	.277	80 (59%)	4 (33.3%)	.088	82 (58.5%)	2 (25%)	.053
Complex	10 (37%)	54 (44.7%)		47 (41%)	17 (51.5%)		56 (41%)	8 (66.7%)		58 (41.5%)	6 (75%)	
Penetrating vessel												
Absent	18 (66.7%)	49 (40.5%)	.023*	53 (46%)	14 (42.4%)	.709	61 (45%)	6 (50%)	.731	64 (45.7%)	4 (50%)	.895
Present	9 (33.3%)	72 (59.5%)		62 (54%)	19 (57.6%)		75 (55%)	6 (50%)		76 (54.3%)	4 (50%)	
Distribution												
Peripheral	20 (74%)	70 (57.8%)	.118	72 (62.6%)	18 (54.5%)	.403	84 (61.8%)	6 (50%)	.424	87 (62.1%)	4 (50%)	.319
Central	7 (26%)	51 (42.2%)		43 (37.4%)	15 (45.5%)		52 (38.2%)	6 (50%)		53 (37.9%)	4 (50%)	
Adler score												
0–1	12 (44.4%)	45 (37.2%)	.487	46 (40%)	11 (33.3%)	.488	54 (39.7%)	3 (25%)	.316	55 (39.3%)	6 (75%)	.177
2–3	15 (55.6%)	76 (62.8%)		69 (60%)	22 (66.7%)		82 (60.3%)	9 (75%)		85 (60.7%)	2 (25%)	
SMI vascular index												
Mean	3.97 ± 5.4	6.57 ± 6.2	.036	5.9 ± 6.4	6.8 ± 5.4	.447	5.39 ± 6	8.2 ± 6.3	.230	5.96 ± 6.1	8.7 ± 6.8	.213
SWE findings	**TIL (−) (*n* = 27)**	**TIL (+) (*n* = 121)**	***p***	**TIL (<) (*n* = 115)**	**TIL (>) (*n* = 33)**	***p***	**TIL (<) (*n* = 136)**	**TIL (>) (*n* = 12)**	***p***	**TIL (<) (*n* = 140)**	**TIL (>) (*n* = 8)**	***p***
SWE findings												
Mean *E*-ratio	11 ± 6.8	13 ± 12.53	.408	12.2 ± 12.7	14.6 ± 7.4	.4312	12.8 ± 12	12.3 ± 5.4	.881	12 ± 6	14.3 ± 6	.399
Mean *E*-mean	115 ± 28.3	112 ± 36.4	.719	107.9 ± 36	130 ± 24.7	.001**	112.9 ± 35.8	112.9 ± 26	.995	115 ± 33	108.5 ± 26.7	.637
Stiff rim sign												
Absent	15 (55.6%)	57 (47.1%)	.427	68 (59%)	4 (12%)	<.001**	69 (50.7%)	3 (4.2%)	.087	69 (49.3%)	4 (50%)	.753
Present	12 (44.4%)	64 (52.9%)		47 (41%)	29 (87.9%)		67 (49.3%)	9 (11.8%)		71 (50.7%)	4 (50%)	

Abbreviations: SMI, super-b microvascular imaging; SWE, shear wave elastography; TIL, tumor infiltrating lymphocyte; VI, vascular index.
*<0.05;
**<0.005.

and attributed this finding to the weak connection between the cells forming TILs.[14,23,27] Eun et al. have investigated the relationship between TILs and tumor stiffness in breast cancer, with a focus on different molecular subtypes in a study that included 803 patients.[28] They also reported that lower tumor stiffness values, as determined by SWE, were significantly associated with higher TIL levels (at 50% level). This inverse correlation was particularly evident in HR(+)/HER-2 negative and TNBC subtypes. Unlike previous reports, our study demonstrated a statistically significant correlation between elevated E-mean values and higher TIL levels at the 10% threshold. This correlation diminished as TIL density continued to rise beyond this level, and no significant elastographic differences were noted at higher TIL levels. In addition, our study showed a significant relationship with stiff rim sign at SWE and TIL positivity at a cut-off level of >10%. The stiff rim sign is markedly increased stiffness around the lesion and is associated with peritumoral desmoplastic stromal reaction, fibrosis, and extracellular matrix accumulation.[39] Recent studies have shown that physical and genetic changes in the stroma surrounding the tumor in breast cancer are effective in tumor growth, tumor extension, immune system defense, and response to therapeutic agents.[27,40] Based on the findings of our study, lymphocyte clusters surrounding the tumor in the peritumoral area may also play a role in the formation of the stiff rim sign up to a certain amount of infiltration.

Varying results reported in the literature indicate that the relationship between tumor stiffness and TIL levels is complex, and tumor stiffness differs based on different molecular subtypes. In addition, the use of different elastography techniques across various machines (e.g., point SWE, 2D-SWE), as well as the consideration of different elastography parameters (such as *E*-mean, *E*-max, *E*-ratio, or elasticity heterogeneity), may have also contributed to the varying

Figure 1. A 49-year-old patient with a palpable mass. **A**, A 21 × 14 mm, irregular hypoechoic mass was observed during the US examination. The mass was hypervascular with Superb microvascular imaging (**B**). In SWE examination (**C**), there was a 'stiff rim' sign around the lesion. The shear waves cannot be observed within the lesion, whereas the periphery shows a rim-like area of increased stiffness. The propagation map of elastography is on the left. The mean E-mean value taken from the perilesional area was measured as 125.3 kPa (**D**). The biopsy result was reported as invasive ductal carcinoma (Grade 2, ER: positive, PR: positive, HER-2: negative, Ki-67: 16%), and the TIL ratio was 15% in the histopathological examination (**E**). Tumor-infiltrating lymphocyte clusters were indicated with an asterisk.

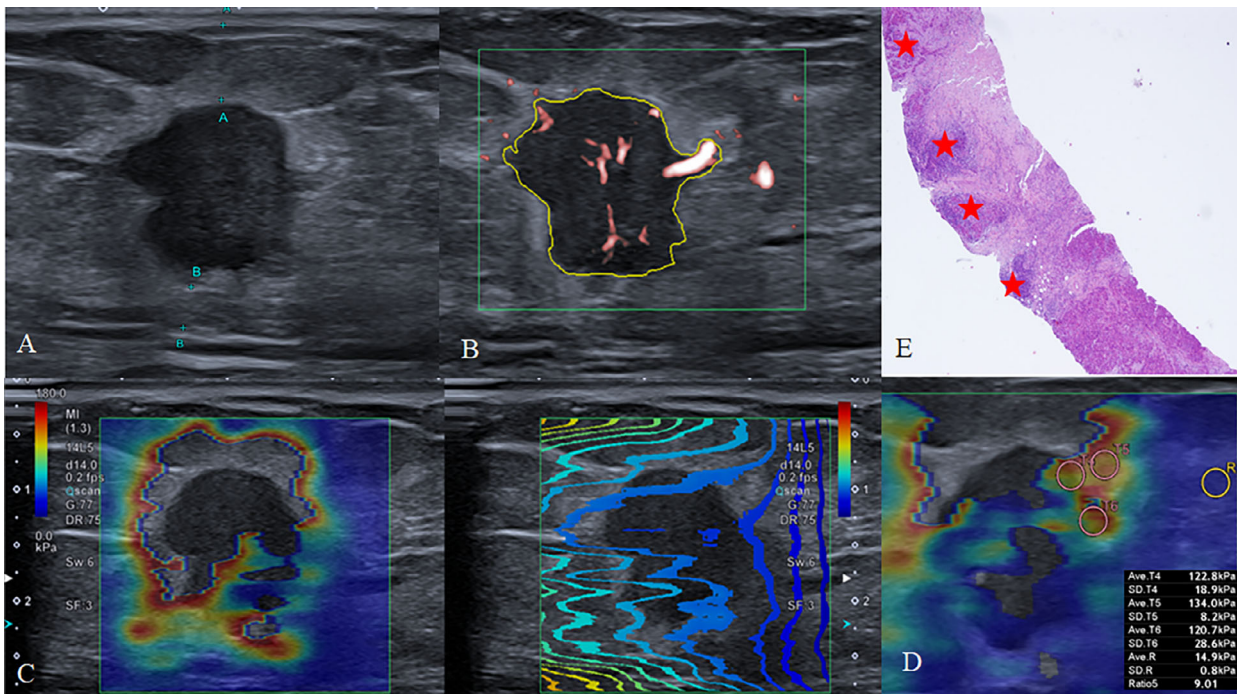

results reported in the literature.[14,23,27,28] Therefore, larger studies that include a higher number of cases of each subtype and a higher number of cases at each cut-off level are needed to reach a definite conclusion on this issue. Our contradicting results may be due to the relatively low number of HER-2 (+) and TNBC in our cohort. Use of different levels could be another reason for the discrepancy between studies. Moreover, the attenuation of correlation at higher TIL levels may reflect a plateau effect, wherein additional lymphocytic infiltration no longer contributes to measurable changes in the mechanical properties of the tumor. These findings highlight the complexity of tumor-immune interactions and suggest that while elastographic parameters may offer insights into the immune microenvironment, their predictive value may be limited to specific TIL ranges or tumor subtypes.

The association between vascularization and TILs has primarily been investigated using less sensitive modalities, such as contrast-enhanced ultrasound (CEUS) and Doppler imaging.[12,13,38] In our study, penetrating vessels and an increased VI, as detected by SMI, were significantly associated with the presence of TILs, suggesting an active immune microenvironment that reflects a high perfusion requirement. While our findings are consistent with those of Jia et al.,[38] who reported more homogeneous and intense enhancement at high TIL levels with CEUS, they differ from studies such as Candelaria et al.;[15] and Fukui et al.[13] This difference may be due to the effects of both the imaging modality used (SMI vs CEUS) and the TIL classification (binary classification of present/absent rather than increasing levels) on the results. Therefore, SMI may better capture subtle neovascularization associated with early immune infiltration. Additionally, a binary classification of TIL levels as present/absent may more accurately reflect the angiogenic response due to immune cell infiltration. These findings suggest that both the imaging technique used and the TIL classification method may influence the detectability of the tumor-related vascular response in breast cancer.

Figure 2. A 67-year-old patient with a palpable mass. B-mode US examination (**A**) shows a 15 × 11 mm, irregular, hypoechoic solid mass. Superb microvascular imaging (**B**) showed a slightly increased vascularization in the lesion. SWE examination (**C**) shows homogeneous color coding around and inside the lesion. The highest elasticity was measured as 47 kPa inside the lesion. The propagation map of elastography is on the left. The result of core-needle biopsy was invasive ductal carcinoma (Grade: II, ER: positive, PR: positive, HER-2: positive, Ki-67 15%). TIL ratio was 1%.

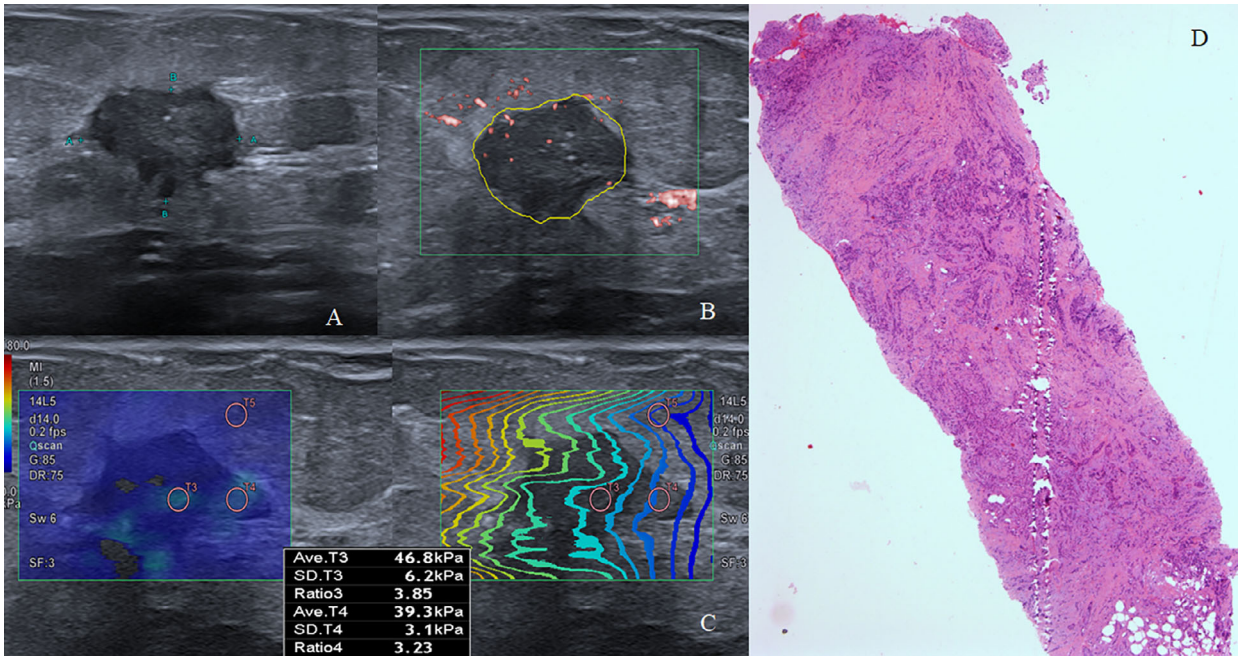

This study has several limitations that should be acknowledged. It is a single-center study, and the data from only one elastography device was used. These may have affected the universality of the study. The number of patients participating in the study is limited. The TIL ratios of the lesions that we included in the study are relatively low. Therefore, further analyses might be needed in larger study populations. In our cohort, the percentage of TNBC and HER-2 positive cases were also relatively low. Larger scale studies are also warranted to validate the applicability of our study results. TIL ratios were evaluated from core-needle biopsy material. The histopathological analysis did not evaluate the degree of fibrosis, desmoplasia, or the amount of collagen in the tissue around the lesion. Additionally, in our study, we were able to evaluate SWE values only as *E*-mean and SWE-ratio because the machine we used does not give the other numeric elasticity parameters. Inter-observer and intra-observer variability were not evaluated in our study. However, the reproducibility of SWE among users has been proven by previous studies.[19]

In conclusion, this multiparametric US study demonstrated significant associations between several morphologic as well as quantitative ultrasound features and TILs in breast cancer. To the best of our knowledge, this is the first study to evaluate the role of SMI in this context, providing preliminary evidence for its potential utility. However, the fact that significance was observed in some parameters only at certain threshold TIL levels indicates that caution should be exercised in the use of these indicators. Inconsistent results across studies may stem from methodological differences, differences in the representation of breast cancer molecular subtypes in cohorts, and varying levels of TILs. Overall, our findings support the utility of non-invasive imaging in reflecting the tumor immune microenvironment in breast cancer. Further comprehensive studies are needed to clarify this relationship.

Data Availability Statement

The data that support the findings of this study are available on request from the corresponding author. The data are not publicly available due to privacy or ethical restrictions.

References

1. Ali HR, Provenzano E, Dawson SJ, et al. Association between CD8+ T-cell infiltration and breast cancer survival in 12,439 patients. *Ann Oncol* 2014; 25:1536–1543. https://doi.org/10.1093/annonc/mdu191.
2. Loi S, Sirtaine N, Piette F, et al. Prognostic and predictive value of tumor-infiltrating lymphocytes in a phase III randomized adjuvant breast cancer trial in node-positive breast cancer comparing the addition of docetaxel to doxorubicin with doxorubicin-based chemotherapy: BIG 02-98. *J Clin Oncol* 2013; 31:860–867. https://doi.org/10.1200/JCO.2011.41.0902.
3. Yamaguchi R, Tanaka M, Yano A, et al. Tumor-infiltrating lymphocytes are important pathologic predictors for neoadjuvant chemotherapy in patients with breast cancer. *Hum Pathol* 2012; 43:1688–1694. https://doi.org/10.1016/j.humpath.2011.12.013.
4. Clark GM. Do we really need prognostic factors for breast cancer? *Breast Cancer Res Treat* 1994; 30:117–126. https://doi.org/10.1007/BF00666054.
5. Savas P, Salgado R, Denkert C, et al. Clinical relevance of host immunity in breast cancer: from TILs to the clinic. *Nat Rev Clin Oncol* 2016; 13:228–241. https://doi.org/10.1038/nrclinonc.2015.215.
6. Denkert C, von Minckwitz G, Brase JC, et al. Tumor-infiltrating lymphocytes and response to neoadjuvant chemotherapy with or without carboplatin in human epidermal growth factor receptor 2-positive and triple-negative primary breast cancers. *J Clin Oncol* 2015; 33:983–991. https://doi.org/10.1200/JCO.2014.58.1967.
7. Bundred NJ. Prognostic and predictive factors in breast cancer. *Cancer Treat Rev* 2001; 27:137–142. https://doi.org/10.1053/ctrv.2000.0207.
8. de Azambuja E, Cardoso F, de Castro G, et al. Ki-67 as prognostic marker in early breast cancer: a meta-analysis of published studies involving 12,155 patients. *Br J Cancer* 2007; 96:1504–1513. https://doi.org/10.1038/sj.bjc.6603756.
9. Fitzgibbons PL, Page DL, Weaver D, et al. Prognostic factors in breast cancer. College of American Pathologists Consensus Statement 1999. *Arch Pathol Lab Med* 2000; 124:966–978. https://doi.org/10.5858/2000-124-0966-PFIBC.
10. Salgado R, Denkert C, Campbell C, et al. Tumor-infiltrating lymphocytes and associations with pathological complete response and event-free survival in HER2-positive early-stage breast cancer treated with Lapatinib and Trastuzumab: a secondary analysis of the NeoALTTO trial. *JAMA Oncol* 2015; 1:448–454. https://doi.org/10.1001/jamaoncol.2015.0830.

11. Khan AM, Yuan Y. Biopsy variability of lymphocytic infiltration in breast cancer subtypes and the ImmunoSkew score. *Sci Rep* 2016; 6:36231. https://doi.org/10.1038/srep36231.
12. Frankowska K, Zarobkiewicz M, Dąbrowska I, Bojarska-Junak A. Tumor infiltrating lymphocytes and radiological picture of the tumor. *Med Oncol* 2023; 40:176. https://doi.org/10.1007/s12032-023-02036-3.
13. Fukui K, Masumoto N, Shiroma N, et al. Novel tumor-infiltrating lymphocytes ultrasonography score based on ultrasonic tissue findings predicts tumor-infiltrating lymphocytes in breast cancer. *Breast Cancer* 2019; 26:573–580. https://doi.org/10.1007/s12282-019-00958-3.
14. Çelebi F, Agacayak F, Ozturk A, et al. Usefulness of imaging findings in predicting tumor-infiltrating lymphocytes in patients with breast cancer. *Eur Radiol* 2020; 30:2049–2057. https://doi.org/10.1007/s00330-019-06516-x.
15. Candelaria RP, Spak DA, Rauch GM, et al. BI-RADS ultrasound lexicon descriptors and stromal tumor-infiltrating lymphocytes in triple-negative breast cancer. *Acad Radiol* 2022; 29:S35–S41. https://doi.org/10.1016/j.acra.2021.06.007.
16. Ku YJ, Kim HH, Cha JH, et al. Correlation between MRI and the level of tumor-infiltrating lymphocytes in patients with triple-negative breast cancer. *AJR Am J Roentgenol* 2016; 207:1146–1151. https://doi.org/10.2214/AJR.16.16248.
17. Barr RG, Nakashima K, Amy D, et al. WFUMB guidelines and recommendations for clinical use of ultrasound elastography: part 2: breast. *Ultrasound Med Biol* 2015; 41:1148–1160. https://doi.org/10.1016/j.ultrasmedbio.2015.03.008.
18. Chae EY, Yoon GY, Cha JH, Shin HJ, Choi WJ, Kim HH. Added value of the vascular index on superb microvascular imaging for the evaluation of breast masses: comparison with grayscale ultrasound. *J Ultrasound Med* 2021; 40:715–723. https://doi.org/10.1002/jum.15441.
19. Evans A, Whelehan P, Thomson K, et al. Differentiating benign from malignant solid breast masses: value of shear wave elastography according to lesion stiffness combined with greyscale ultrasound according to BI-RADS classification. *Br J Cancer* 2012; 107:224–229.
20. Chang JM, Moon WK, Cho N, et al. Clinical application of shear wave elastography (SWE) in the diagnosis of benign and malignant breast diseases. *Breast Cancer Res Treat* 2011; 129:89–97. https://doi.org/10.1007/s10549-011-1627-7.
21. Sohn YM, Seo M. Breast lesions diagnosed by ultrasound-guided core needle biopsy: can shearwave elastography predict histologic upgrade after surgery or vaccuum assisted excision? *Clin Imaging* 2018; 49:150–155. https://doi.org/10.1016/j.clinimag.2018.03.004.
22. Au FWF, Ghai S, Lu FI, Moshonov H, Crystal P. Quantitative shear wave elastography: correlation with prognostic histologic features and immunohistochemical biomarkers of breast cancer. *Acad Radiol* 2015; 22:269–277.
23. Li J, Sun B, Li Y, et al. Correlation analysis between shear-wave elastography and pathological profiles in breast cancer. *Breast Cancer Res Treat* 2023; 197:269–276. https://doi.org/10.1007/s10549-022-06804-z.
24. Berg WA, Mendelson EB, Cosgrove DO, et al. Quantitative maximum shear-wave stiffness of breast masses as a predictor of histopathologic severity. *AJR Am J Roentgenol* 2015; 205:448–455. https://doi.org/10.2214/AJR.14.13448.
25. Youk JH, Gweon HM, Son EJ, Kim JA, Jeong J. Shear-wave elastography of invasive breast cancer: correlation between quantitative mean elasticity value and immunohistochemical profile. *Breast Cancer Res Treat* 2013; 138:119–126.
26. Crnogorac M, Ivanac G, Tomasović-Lončarić Č, Žic R, Kelava T, Brkljačić B. Sonoelastographic features of high-risk breast lesions and ductal carcinoma in situ – a pilot study. *Acta Clin Croat* 2019; 58:13–22. https://doi.org/10.20471/acc.2019.58.01.02.
27. Lee Y, Bae SJ, Eun NL, Ahn SG, Jeong J, Cha YJ. Correlation of yes-associated protein 1 with stroma type and tumor stiffness in hormone-receptor positive breast cancer. *Cancers* 2022; 14:4971. https://doi.org/10.3390/cancers14204971.
28. Eun NL, Bae SJ, Youk JH, et al. Tumor-infiltrating lymphocyte level consistently correlates with lower stiffness measured by shear-wave elastography: subtype-specific analysis of its implication in breast cancer. *Cancers* 2024; 16:1254. https://doi.org/10.3390/cancers16071254.
29. Lee EJ, Chang YW. Combination of quantitative parameters of shear wave elastography and superb microvascular imaging to evaluate breast masses. *Korean J Radiol* 2020; 21:1045–1054. https://doi.org/10.3348/kjr.2019.0765.
30. Kayadibi Y, Kargin OA, Aladag Kurt S, Ozturk T, Yilmaz MH. Pilot study to evaluate the association between superb microvascular imaging (SMI) and histologic markers of angiogenesis in patients with invasive ductal carcinoma. *J Ultrasound Med* 2025; 44:1201–1211. https://doi.org/10.1002/jum.16674.
31. Krüger K, Silwal-Pandit L, Wik E, et al. Baseline microvessel density predicts response to neoadjuvant bevacizumab treatment of locally advanced breast cancer. *Sci Rep* 2021; 11:3388. https://doi.org/10.1038/s41598-021-81914-0.
32. Park AY, Kwon M, Woo OH, et al. A prospective study on the value of ultrasound microflow assessment to distinguish malignant from benign solid breast masses: association between ultrasound parameters and histologic microvessel densities. *Korean J Radiol* 2019; 20:759. https://doi.org/10.3348/kjr.2018.0515.
33. Sickles EA, D'Orsi CJ, Bassett LW, Appleton CM, Berg WA, Burnside ES. *ACR BI-RADS® Atlas, Breast Imaging Reporting and Data System*. Reston, VA: American College of Radiology; 2013: 39-48.

34. Adler DD, Carson PL, Rubin JM, Quinn-Reid D. Doppler ultrasound color flow imaging in the study of breast cancer: preliminary findings. *Ultrasound Med Biol* 1990; 16:553–559.
35. Parise CA, Bauer KR, Brown MM, Caggiano V. Breast cancer subtypes as defined by the estrogen receptor (ER), progesterone receptor (PR), and the human epidermal growth factor receptor 2 (HER2) among women with invasive breast cancer in California, 1999–2004. *Breast J* 2009; 15:593–602. https://doi.org/10.1111/j.1524-4741.2009.00822.x.
36. Salgado R, Denkert C, Demaria S, et al. The evaluation of tumor-infiltrating lymphocytes (TILs) in breast cancer: recommendations by an international TILs working group 2014. *Ann Oncol* 2015; 26:259–271. https://doi.org/10.1093/annonc/mdu450.
37. Fogante M, Tagliati C, De Lisa M, Berardi R, Giuseppetti GM, Giovagnoni A. Correlation between apparent diffusion coefficient of magnetic resonance imaging and tumor-infiltrating lymphocytes in breast cancer. *Radiol Med* 2019; 124:581–587. https://doi.org/10.1007/s11547-019-01008-w.
38. Jia Y, Zhu Y, Li T, et al. Evaluating tumor-infiltrating lymphocytes in breast cancer: the role of conventional ultrasound and contrast-enhanced ultrasound. *J Ultrasound Med* 2023; 42:623–634. https://doi.org/10.1002/jum.16058.
39. Evans A, Whelehan P, Thomson K, et al. Invasive breast cancer: relationship between shear-wave elastographic findings and histologic prognostic factors. *Radiology* 2012; 263:673–677. https://doi.org/10.1148/radiol.12111317.
40. Andre F, Berrada N, Desmedt C. Implication of tumor microenvironment in the resistance to chemotherapy in breast cancer patients. *Curr Opin Oncol* 2010; 22:547–551. https://doi.org/10.1097/CCO.0b013e32833fb384.